Supporting Information for

Intra-wire coupling in segmented Ni/Cu nanowires deposited by electrodeposition

By

Philip Sergelius, Ji Hyun Lee, Olivier Fruchart, Mohamed Shaker Salem, Sebastian Allende, Roberto Escobar, Johannes Gooth, Robert Zierold, Jean-Christophe Toussaint, Sebastian Schneider, Darius Pohl, Bernd Rellinghaus, Sylvain Martin, Javier Garcia, Heiko Reith, Anne Spende, Maria Eugenia Toimil-Molares, Dora Altbir, Russel Cowburn, Detlef Görlitz, Kornelius Nielsch

Nanotechnology, 2016
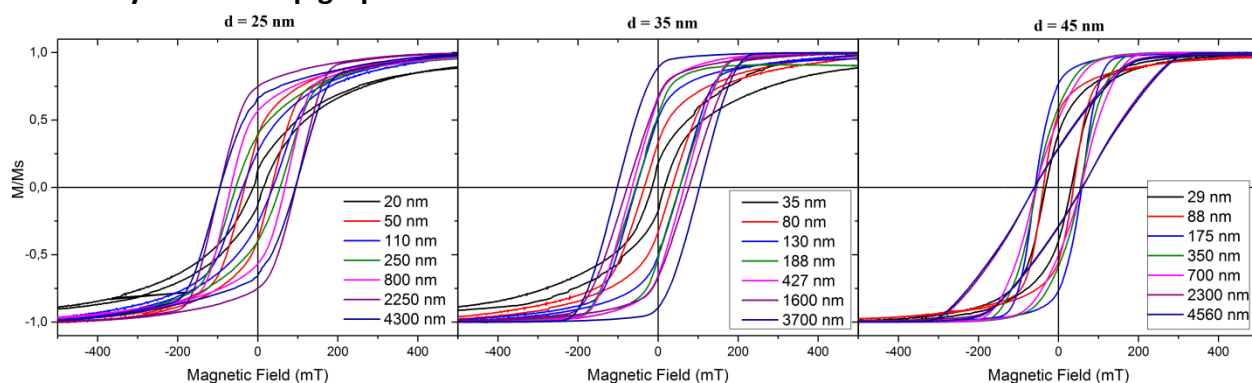
1. Hysteresis loop graphs

Figure SI-1 Hysteresis loops for all diameters and lengths acquired using a VSM. To obtain sufficient signal strength for the shortest wires, some membrane pieces were stacked. The total membrane thickness is 50 µm, which means that interactions between the stacked membrane pieces can be neglected.

2. Aspect ratio dependent First-Order Reversal Curve (FORC) analysis of d=45 nm nanowires

First order reversal curves are often used to investigate dipolar interactions within nanowire arrays. For a detailed description of the underlying method, refer to the references [1-5]. The FORC diagrams presented here were obtained using the *FORCinel* package by Harrison and Feinberg [6]. Figure Figure SI-2 shows the FORC diagrams for d=25 nm, d= 35 nm and d=45 nm nanowires. Qualitatively, the elongation along the interaction field axis (H_u) increases with

increasing wire diameter, as expected. Note that the interpore distance of 105 nm is constant. Varying shapes from "wishbone" shaped structures for the thinnest wires up to elongated shapes for the thickest wires are observed. Several publications have been written on how to extract quantitative information from a FORC diagram [3,4,7,1] and shall therefore not be elaborated in this study anymore.
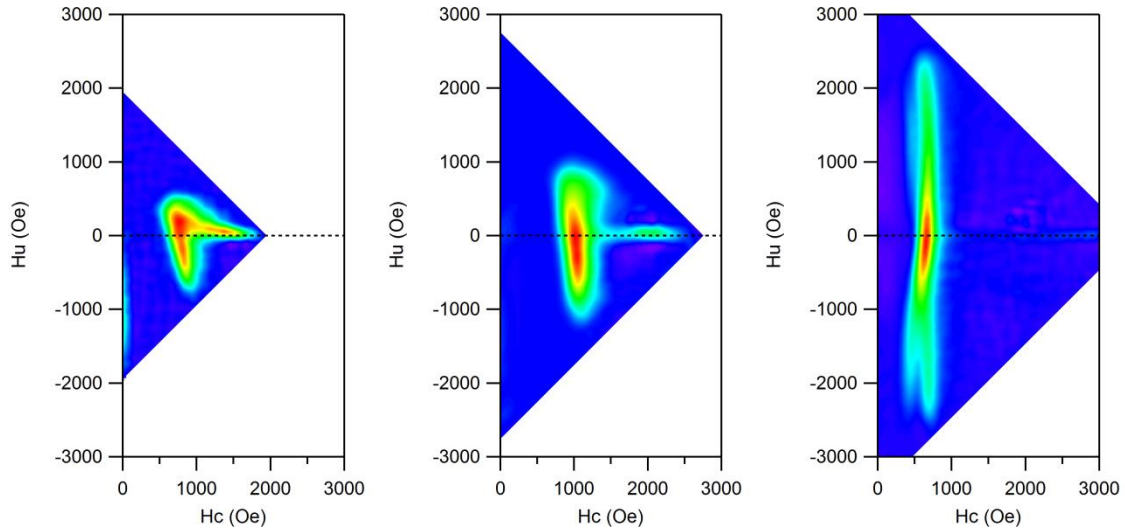

Figure SI-2 FORC diagrams for d = 25 nm, d = 35 nm and d=45 nm nanowires with lengths of approx. 4 µm each (left to right). ($\vec{B}$||wire axis)

Figure SI-3 shows the length dependence of the FORC diagram for the d = 45 nm nanowires. As expected, a qualitative increase of the shape elongation along the interaction field axis (H_u) can be observed. This behavior is expected, because a longer cylinder causes a larger stray field (compare Eq. 1 from the manuscript). The saturation – there is no quantitative difference between 2300 nm and 4560 nm - for the longest nanowires is due to the saturation of demagnetizing field, which has an absolute value that is identical to the stray field.
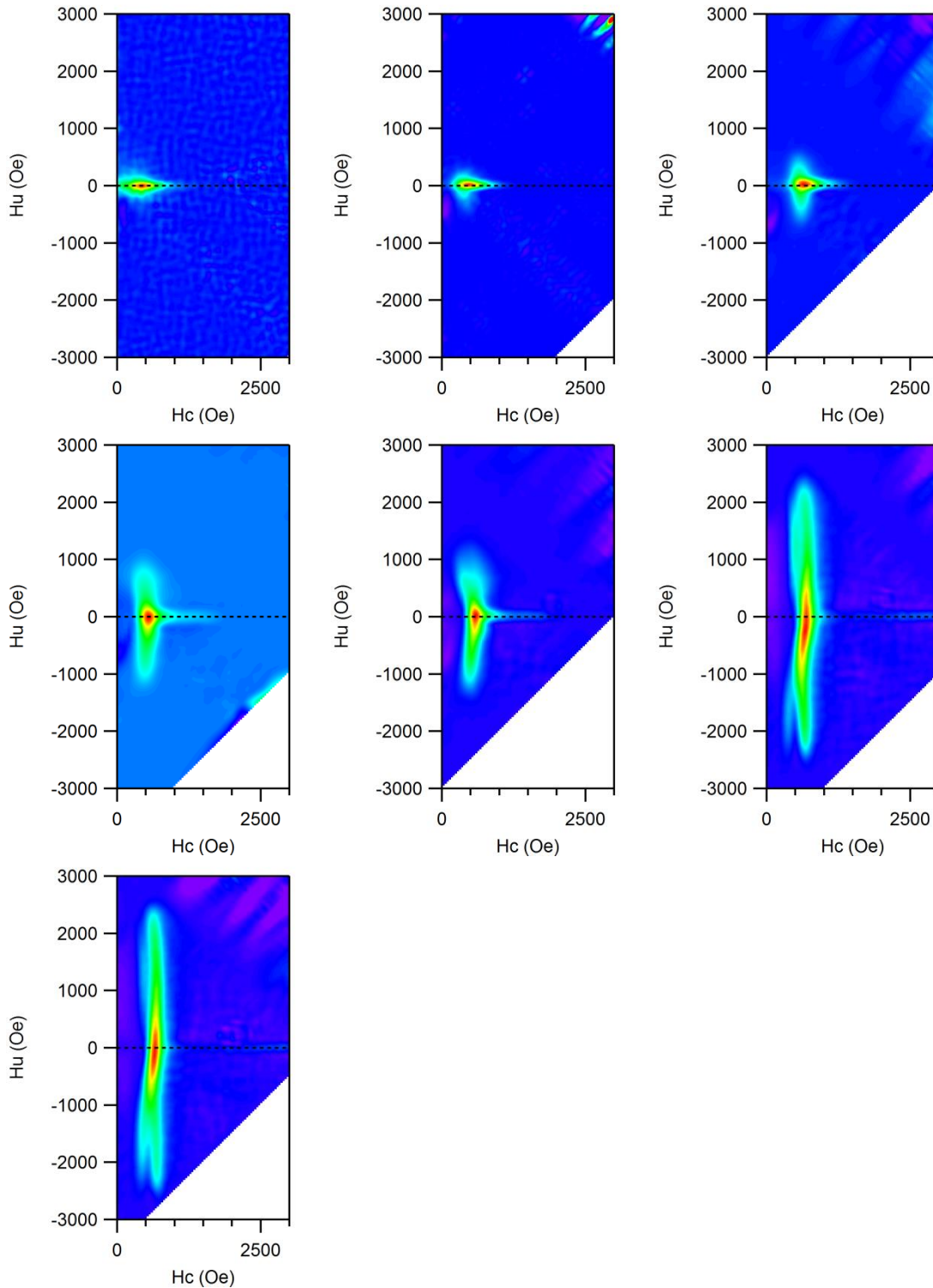
Figure SI-3 FORC diagrams for the d = 45 nm nanowires for lengths of 29 nm, 88 nm, 175 nm, 350 nm, 700 nm, 2300 nm and 4560 nm (top left to bottom right). ($\vec{B}$||wire axis).

3. R vs T graphs for all diameters

The wires are contacted using optical lithography in a four-probe geometry and sputtering. The lengths of the measured nanowires are defined by the distance between both inner contacts, which is on the order of 2-4 µm. The measurement mode is AC using a lock-in at approx. 12.1 Hz and 200 nA current.
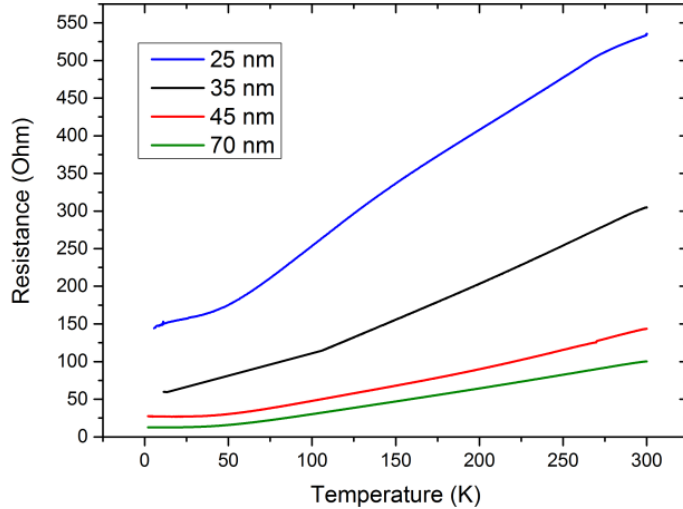

Figure SI-4 Nearly linear R vs T dependences indicate good metallic quality with residual resistivity ratios around 4.5. Slight curvatures, especially observed in the 25 nm case, are due to an inhomogeneous heating rate of the cryostat, because the measurements are taken in sweeping mode and the nanowire itself and the substrate need a few minutes to be in a thermally relaxed state. The IV-relations are linear in all cases and for all temperatures (not shown).

4. Figure for determination of alpha for phase diagrams

For the determination of an analytical model between two interacting, cylindrical ferromagnetic segments, it is important to find out how the nucleation volume size affects switching behaviors. In a simple picture, the stray field (Eq. 1) of one segment reaches into the volume of the other segment by a certain amount, reflecting the nucleation volume. Figure SI-5 evaluates the scaling law presented in Eq. 2. The axis intercept gives the size of the phenomenological parameter $2\alpha = 1$. The model predicts a slope of 1, which is well represented in the graph, which hints at its robustness.
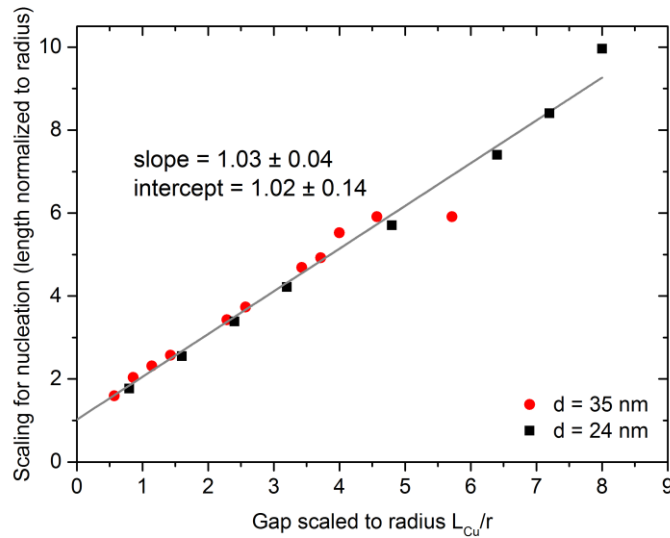

Figure SI-5 Simulated variation of the stray field versus the gap size between two magnetic segments, normalized to their radius.

5. MFM image of two nanomagnets

For capturing the MFM images, the nanowires were saturated in one direction first with the tip removed. The scan was performed in zero field. Further MFM experiments with low moment tips are planned to elucidate the switching behavior of the coupled segments.
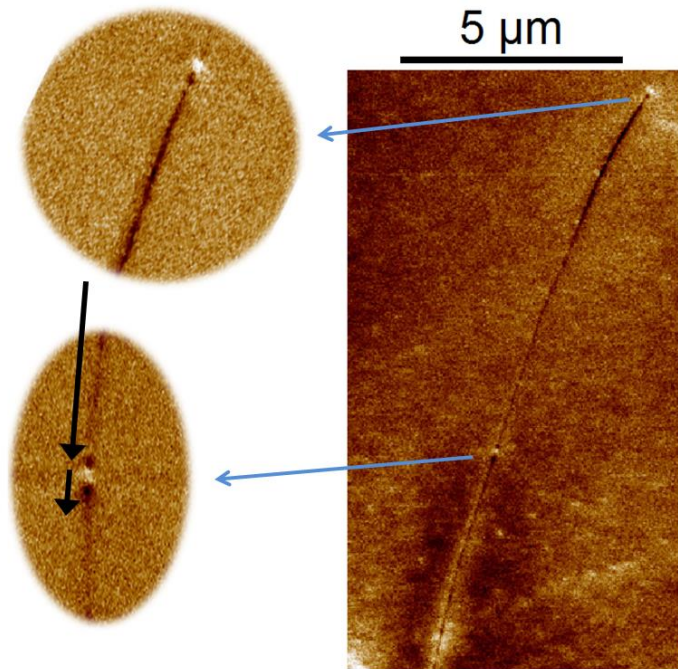

Figure SI-6 MFM image of a long nanomagnet (5 μm, top) and a short (150 nm, bottom). White-Black-White-Black contrast (from top to bottom) indicates a parallel orientation of both segments.

6. Elemental analysis of the segmented nanowires

The nanowires are grown from one electrolyte. TEM-EDS scans are conducted in the respective regions to confirm a Ni-Cu-Ni interface region.
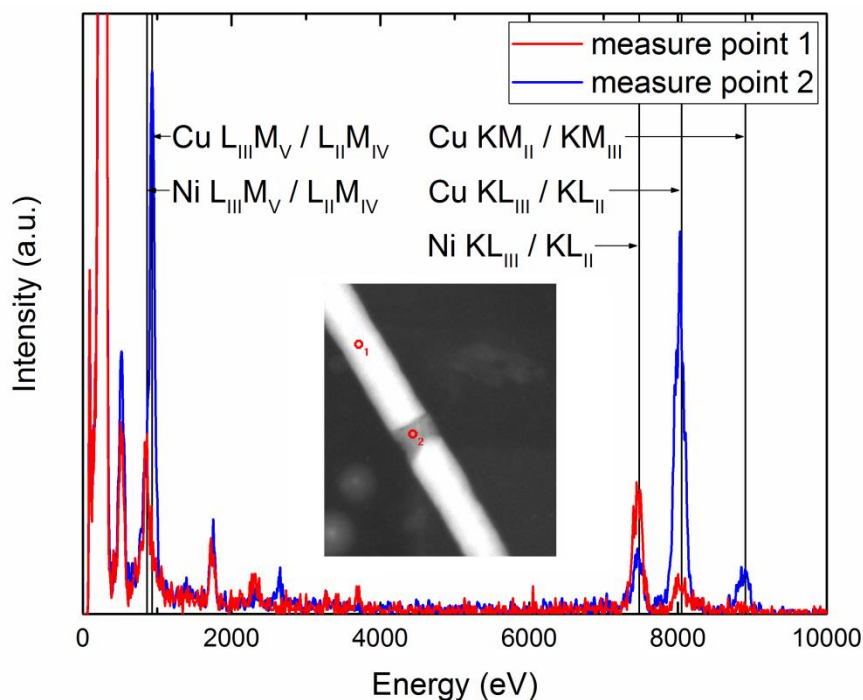
Figure SI-7 TEM-EDS elemental analysis confirming that the dark region is copper, whereas the bright is nickel.

[1]   Sergelius, P.; Fernandez, J. G.; Martens, S.; Zocher, M.; Bohnert, T.; Martinez, V. V.; de la Prida, V. M.; Gorlitz, D.; Nielsch, K. *Journal of Physics D-applied Physics* **2016**, *49*, 145005.

[2]   Mayergoyz, I. D. *J. Appl. Phys.* **1985**, *57*, 3803–3805.

[3]   Beron, F.; Carignan, L.-P.; Menard, D.; Yelon, A. In *Electrodeposited Nanowires and Their Applications*; Lupu, N., Ed.; INTECH, Croatia, 2010; Chapter Ch. 7: "Extracting Individual Properties from Global Behaviour: First-order Reversal Curve Method Applied to Magnetic Nanowire Arrays", pp 167–188.

[4]   Dobrota, C.-I.; Stancu, A. *J. Appl. Phys.* **2013**, *113*, 043928.

[5]   Proenca, M. P.; Ventura, J.; Sousa, C. T.; Vazquez, M.; Araujo, J. P. *J. Phys.: Condens. Matter* **2014**, *26*, 116004.

[6]   Harrison, R. J.; Feinberg, J. M. *Geochem., Geophys., Geosyst.* **2008**, *9*, 1–11.

[7]   Dobrota, C.-I.; Stancu, A. *Physica B* **2015**, *457*, 280–286.